A Comparative Study of Experiments and Calculations on the Polymorphisms of 2,4,6,8,10,12-Hexanitro-2,4,6,8,10,12-hexaazaisowurtzitane (CL-20) Precipitated by Solvent/Anti-solvent Method

Xianfeng Wei, Jinjiang Xu, Hongzhen Li, Xinping Long, and Chaoyang Zhang*

Institute of Chemical Materials, China Academy of Engineering Physics (CAEP), P. O. Box 919-327, Mianyang, Sichuan 621900, China.

Supporting Information (SI)

Table of Contents

S1. Representation of the molecular conformations of CL-20.

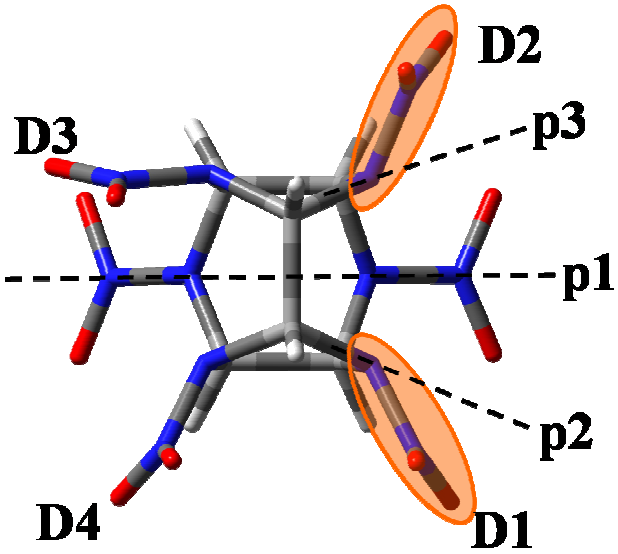

Figure s1. Plot showing axially or equatorially oriented NO_2 groups and numbering of C-C-N-N dihedrals. Three planes are found in the *α*-formed conformation of CL-20, namely, **p1** across the middle of the molecule, and **p2** and **p3** of CCN planes. In D1 (a CCNN dihedral), the N-NO_2 group deviates from **p1** relative to **p2**, so the NO_2 group is inferred to be axially oriented (*a*). Similarly, the NO_2 groups in D2 and D3 within 90° to 180° are axially oriented, and those within -180° to -90° are equatorially oriented (*e*).

We investigated the effects of solvent on the dynamic behavior of the CL-20 molecules, in particular the NO_2 groups. We distinguished the orientations of NO_2 groups and molecular conformations, which are important for MD analysis. The orientation of any NO_2 group in the molecule relative to a plane was determined by two C atoms and one N atom, which links the two C atoms and NO_2 group. Thus, a CCNN dihedral was confirmed.

S2. Abbreviations, dielectric constants and dipoles of the discussed solvents.

Table s1. Abbreviations, dielectric constants and dipoles of the discussed solvents.

Objects	Abbreviation	Dielectric constant	Dipole, Debye
Water	W	78.39	1.94
Acetone	ACE	20.70	2.72
Dichloromethane	DCM	8.93	1.71
Dichloroethane	DCE	10.36	2.74
Acetic ether	AE	6.02	1.88
Heptane	HE	1.92	0.06
Tetrachloromethane	TCM	2.228	0
Cyclohexane	CH	2.023	0
Toluene	TOL	2.379	0.38
Single Molecule	GAS	-	-

S3. Verifying the validation of COMPASS force field to the related systems by comparing experimental and predicted densities, and the detailed MD simulations.

Table s2. Comparison of experimental and predicted densities (in g/cm^3) of the solvents at 298 K, and the predicted densities of amorphous systems with a CL-20 molecule surrounded by 200 solvent molecules at 298 and 350 K.

Solvent	$\rho_{exp,\ 298K}$	$\rho_{simul,\ 298K}$	Relative error, %	$\rho_{solvent+CL\text{-}20,\ 298K}$	$\rho_{solvent+CL\text{-}20,\ 350K}$
DCM	1.330	1.288	3.16	1.301	1.205
DCE	1.260	1.310	-3.97	1.322	1.266
TOL	0.866	0.877	-1.27	0.888	0.841
EA	0.902	0.909	-0.78	0.920	0.861
ACE	0.791	0.804	-1.64	0.821	0.762
CH	0.779	0.777	0.26	0.787	0.737
HE	0.710	0.695	2.11	0.861	0.669
W	1.000	0.970	3.00	1.078	1.053
TCM	1.594	1.671	-4.83	1.695	1.617

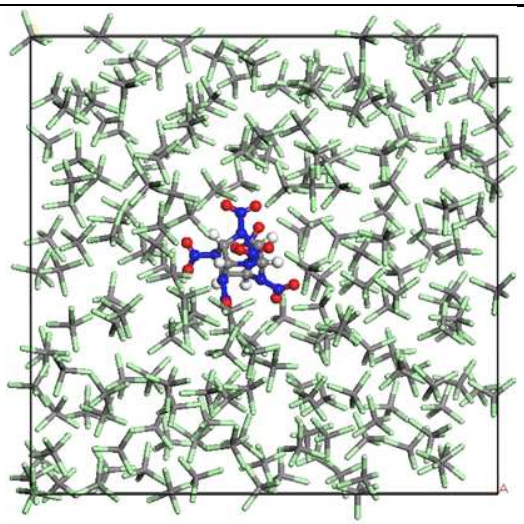

Figure s2. An amorphous cell with a CL-20 molecule (solute) encompassed by 200 solvent molecules (TCM) for MD simulations.

Table s2 lists the predicted densities of amorphous systems with a CL-20 molecule surrounded by 200 solvent molecules at 298 and 350 K. The amorphous cell containing a CL-20 molecule and 200 solvent molecules shown in Figure s2 were equilibrated by *NPT* simulations, with each simulation for 10 ns with a time step of 1 fs. The dynamic trajectories were recorded every 1000 fs, that is, 10000 frames were recorded. The final equilibrated 1000 frames were used for dynamic analyses of densities. We confirmed the equilibration of the final frames and selected a frame with an assembly average of density for the following *NVT* simulations. Each *NVT* simulation lasted for 10 ns with a time step of 1 fs. Dynamic trajectories were recorded per 1 ps, and final 1 ns was used

for dynamic analyses for molecular conformations. Subsequently, we ascertained the distributions of the interesting molecular conformations from these 1000 frames according to the four dihedrals, namely, D1, D2, D3, and D4 (Figure s1).

S4. Verifying the dynamically equilibrated structures, the statistic meanings and equilibrated CL-20 molecular structures independent on the initial ones.

Before analyzing the MD simulation results, we completed two tasks: one is to verify that data are from dynamically equilibrated structures and of statistic meanings; the other is to confirm whether the equilibrated CL-20 molecular structures are dependent on the initial ones or not. To verify that the data are of a statistic meaning, we continued the *NVT* MD simulation for another 9 ns on an equilibrated box with a CL-20 molecule and 200 TCM molecules. As a result, it shows that the data of the final 1 ns of the 10 ns *NVT* simulation are statistically meaningful enough as indicated in Table s3, in that there are very close occurrences of α (γ), β and ε-formed MCs and their sums within every 1 ns. That is, the structures of the final 1 ns have been already equilibrated and all data derived from them are reliable. Also, one can see that the α (γ), β and ε-forms dominate the conformations in crystals at the ambient conditions, but appear in gas or solutions with about a half of the total amount of occurrences, suggesting almost an equal total amount of other conformational forms besides α (γ), β and ε-ones. It shows that the conformational transformation in solutions happen easily, same as the case in the supposed gaseous state[12,24,25].

Table s3. Occurrences of α (γ), β and ε-formed MCs and their sums in TCM at 298 K.

Frame	α	β	ε	$\alpha+\beta+\varepsilon$
1-1000	0.101	0.306	0.099	0.506
1001-2000	0.101	0.321	0.123	0.545
2001-3000	0.117	0.338	0.123	0.578
3001-4000	0.088	0.357	0.119	0.564
4001-5000	0.079	0.327	0.112	0.518
5001-6000	0.086	0.320	0.112	0.518
6001-7000	0.112	0.325	0.114	0.551
7001-8000	0.112	0.317	0.115	0.544
8001-9000	0.089	0.355	0.101	0.545
9001-10000	0.125	0.301	0.127	0.553
Average	0.101	0.327	0.115	0.542

Secondly, we carried out separately the MD simulations for 10 ns on a box composed of one CL-20 molecule and 200 TCM molecules with initial α (γ), β or ε-formed conformations to make sure whether the CL-20 molecular structures are dependent on the initial ones or not. According to

the definition illustrated in Figure s1, the conformational distributions can be confirmed by dihedral (D1 to D4) analyses. As shown in Table s4, firstly, we find that these distributions are independent on the conformational forms of initial CL-20 molecules. That is to say, there are approximately equal distributions of *e* or *a*-formed orientations in all dihedrals, no matter α (γ), β or ε-formed conformation was set to the CL-20-solvent amorphous cell initially. It also suffices to evidence that the CL-20 molecule is dynamically equilibrated in the solvent. In addition, it accords with the static quantum chemical results, which show there are only several kJ/mol energy barriers for NO_2 group reversion. Namely, these very low energy barriers are so easily overcome that all CL-20 molecules have similar MC distributions regardless their initial conformations.

Table s4. Distribution fractional of *e* and *a*-orientationed NO_2 groups in CL-20 conformations in TCM at 298 K as the initial conformation is different as α (γ), β and ε-forms.

Initial conformation	D1		D2		D3		D4	
	e	*a*	*e*	*a*	*e*	*a*	*e*	*a*
α (γ)	0.57	0.43	0.62	0.38	0.54	0.46	0.65	0.35
β	0.55	0.45	0.62	0.38	0.59	0.41	0.62	0.38
ε	0.55	0.45	0.58	0.42	0.58	0.42	0.64	0.36

S5. Experimental results of EA/DCM, EA/TOL, EA/CH and EA/HE precipitation.

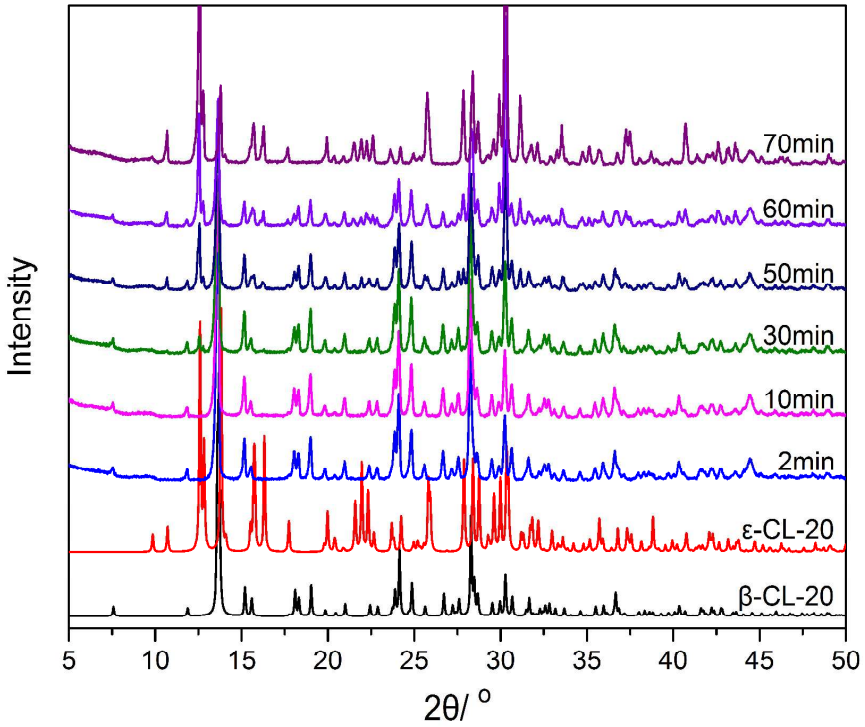

Figure s3. PXRD pattern evolution of CL-20 precipitated from EA/DCM at room temperature.

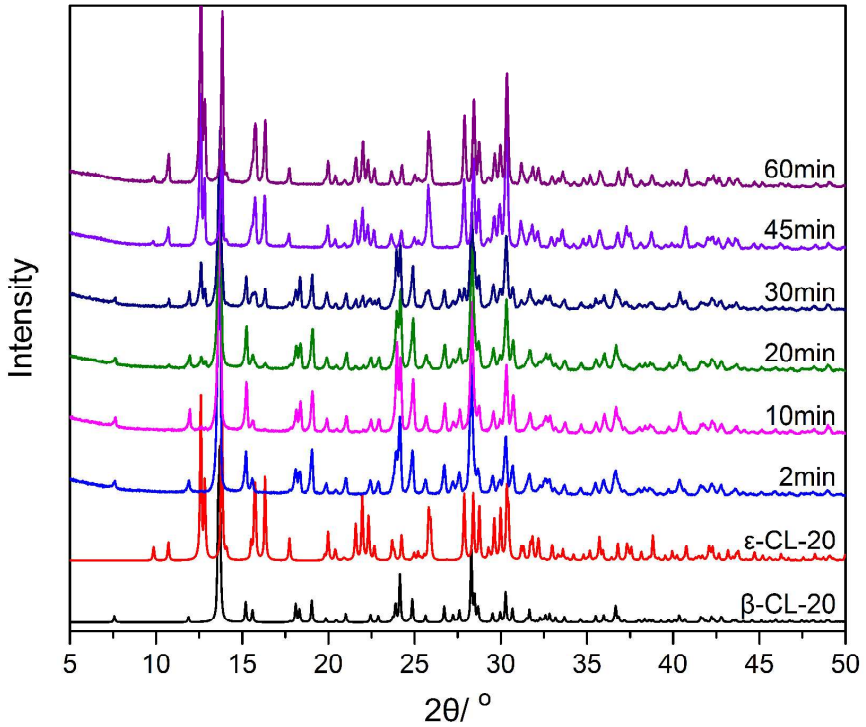

Figure s4. PXRD pattern evolution of CL-20 precipitated from EA/TCM at room temperature.

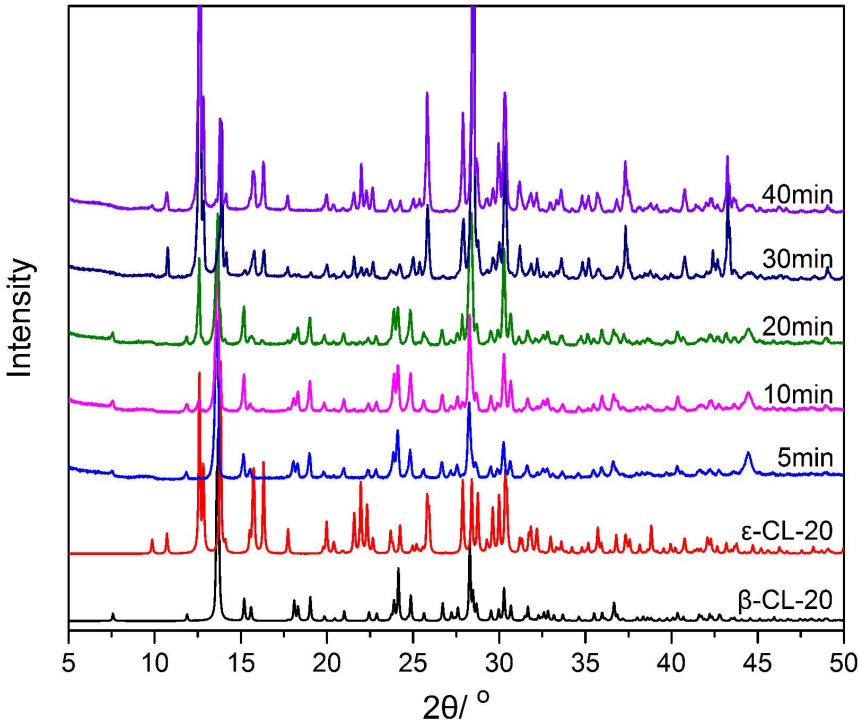

Figure s5. PXRD pattern evolution of CL-20 precipitated from EA/CH at room temperature.

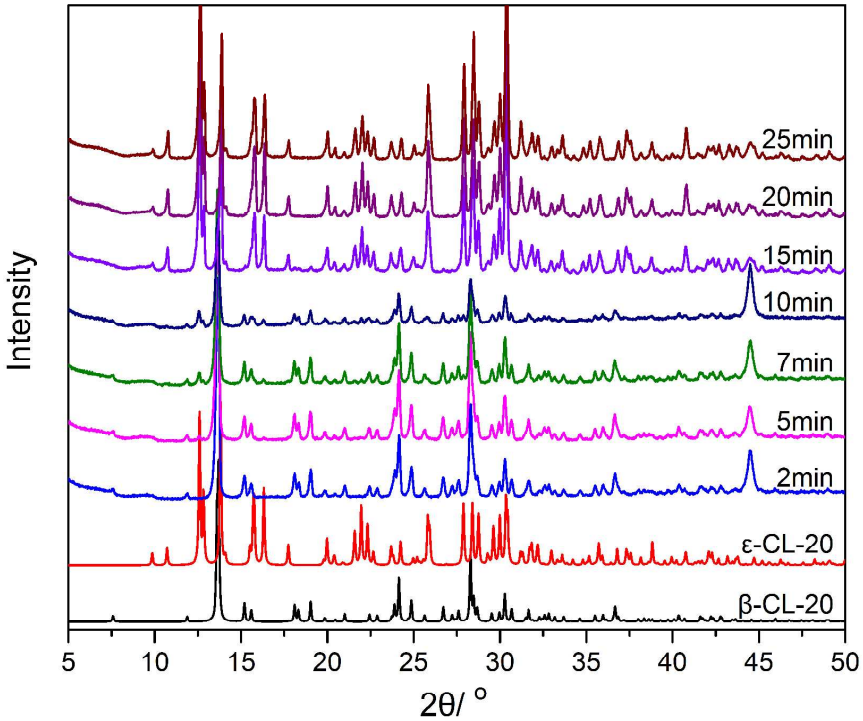

Figure s6. PXRD pattern evolution of CL-20 precipitated from EA/HE at room temperature.

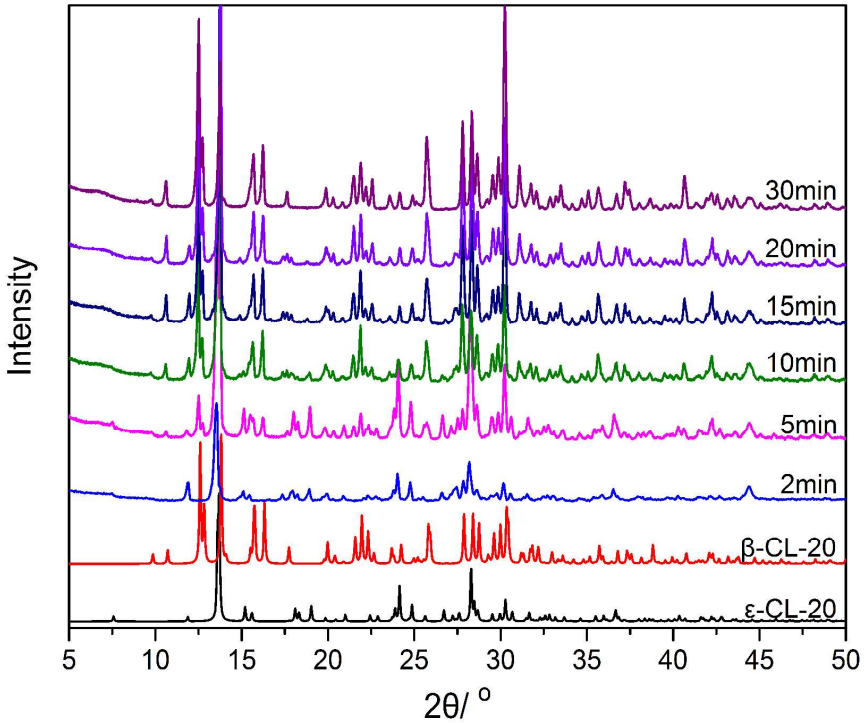

Figure s7. PXRD pattern evolution of CL-20 precipitated from EA/TOL at room temperature.

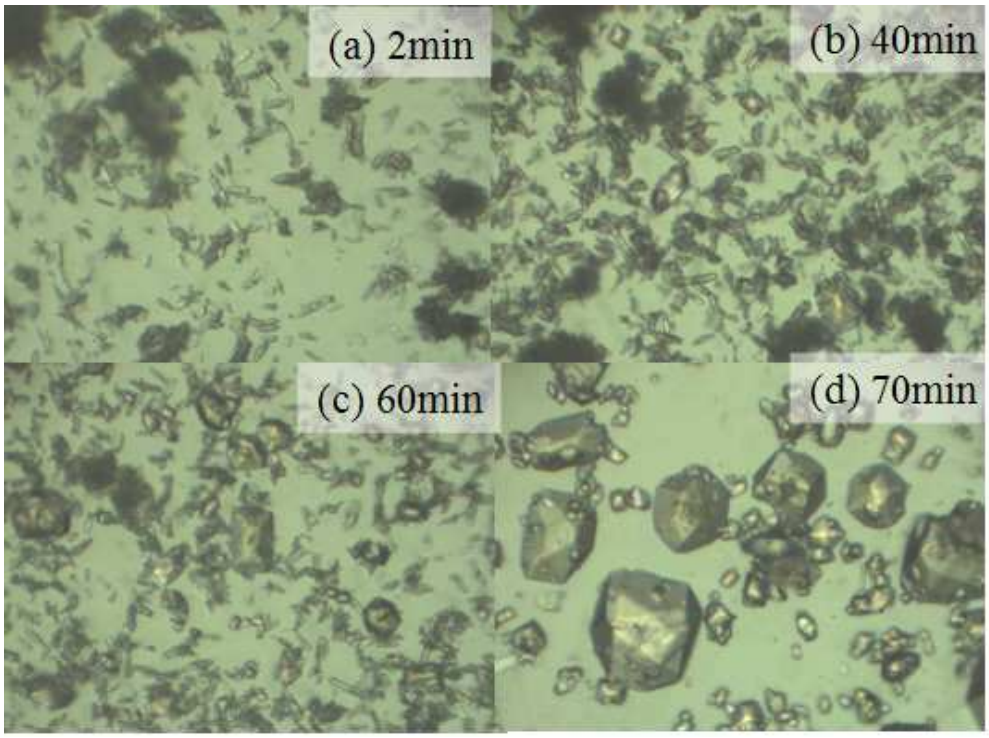

Figure s8. Microscopic image evolution of CL-20 precipitated from EA/DCM at room temperature.

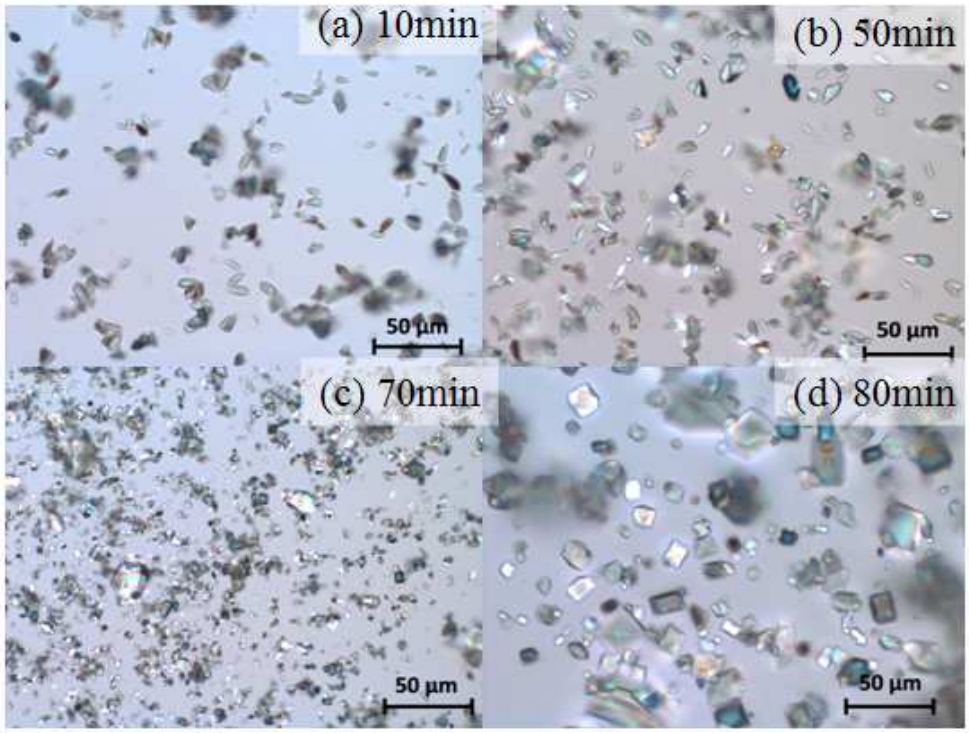

Figure s9. Microscopic image evolution of CL-20 precipitated from EA/HE at room temperature.

S6. Molecular properties.

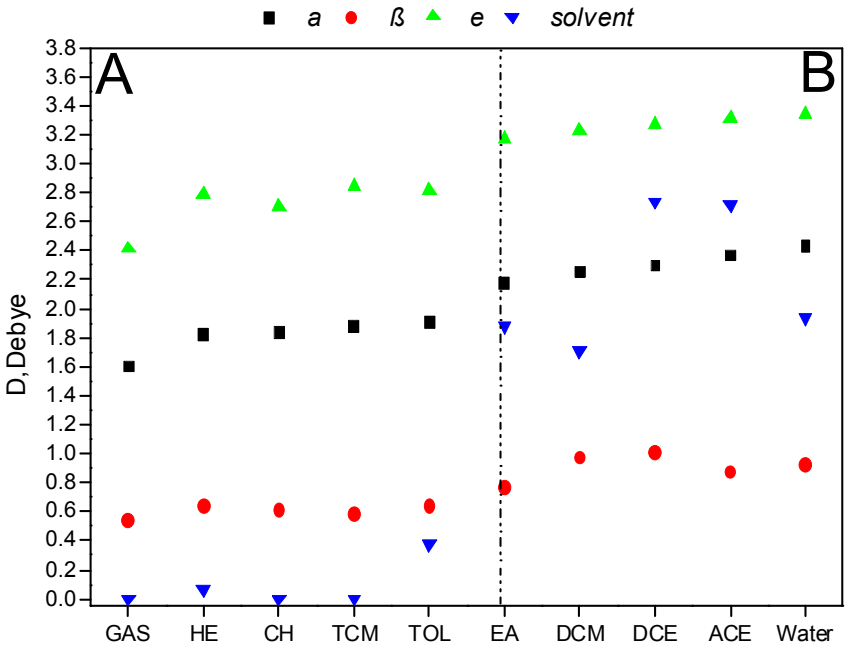

Figure s10. Dipole moments of three interesting CL-20 conformations in various solvents and of solvents themselves.

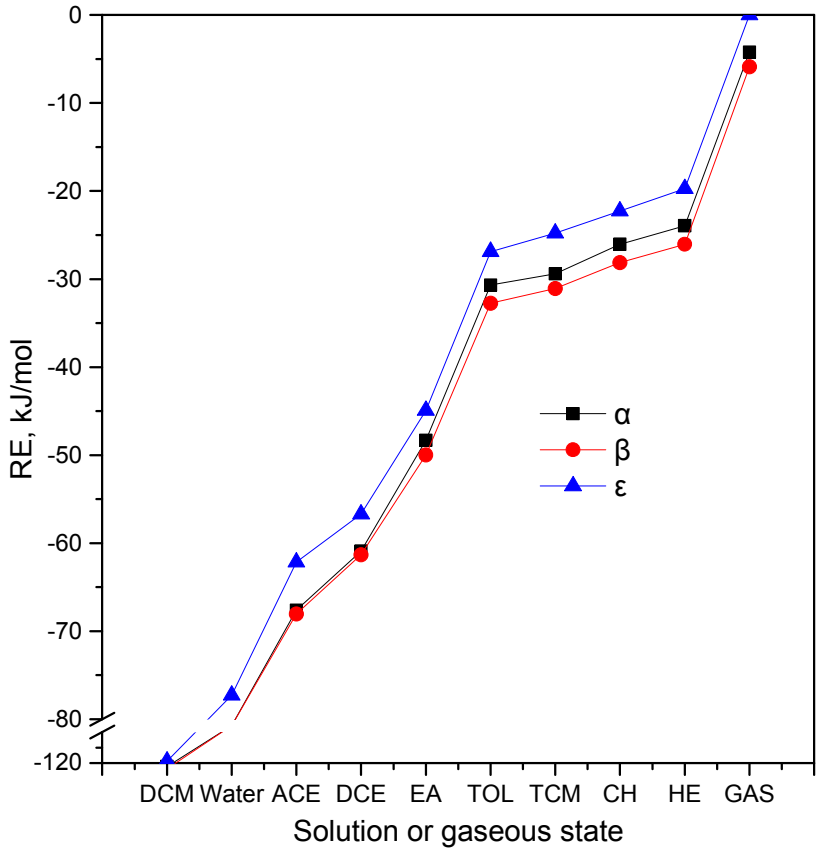

Figure s11. Relative energy (RE) of three interesting CL-20 conformations in different solvents and gaseous state to gaseous ε-CL-20.

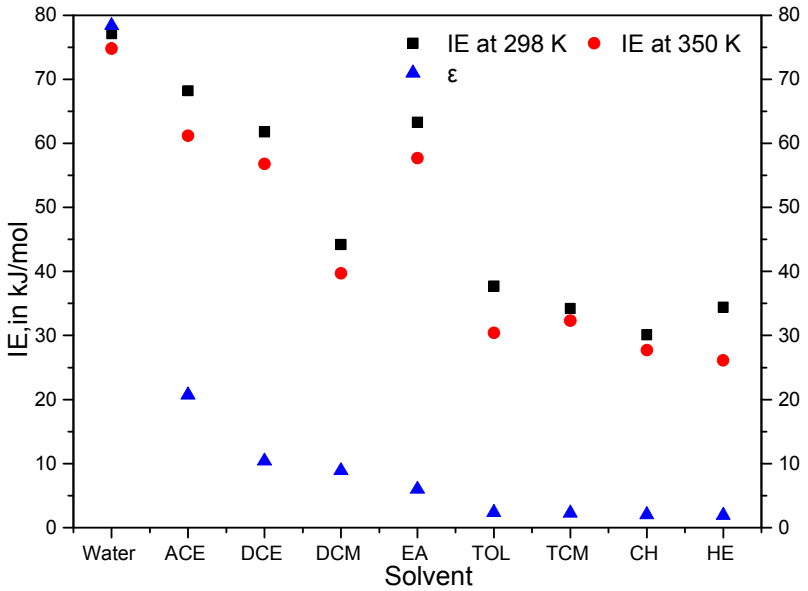

Figure s12. Interaction energies (IEs, in kcal/mol) between CL-20 molecule and solvent molecules surrounding it at 298 and 350 K and dielectric constants (εs) of the solvents.

S7. Verifying Distribution ranges of the related dihedrals and Distribution fractional of *e* and *a*-formed NO_2 groups in the CL-20 conformations in solvents at 298 and 350 K.

Table s5. Distribution ranges of the related dihedrals.

Ranges of Dihedrals	D1		D2		D3		D4	
	D	S	D	S	D	S	D	S
GAS_298K	-113, 120	127	-110, 119	131	-109, 119	132	-108, 119	133
GAS_350K	-108, 119	133	-108, 119	133	-108, 119	133	-108, 119	133
TCM_298K	-113, 127	120	-116, 129	115	-115, 128	116	-116, 128	116
TCM_350K	-111, 125	124	-112, 124	124	-110, 119	131	-109, 126	125
ACE_298K	-118, 128	114	-114, 131	115	-118, 126	116	-119, 130	111
ACE_350K	-115, 130	115	-118, 127	115	-118, 126	116	-115, 127	118
DCE_298K	-116, 130	114	-117, 130	113	-118, 132	110	-120, 130	110
DCE_350K	-112, 130	118	-111, 130	119	-113, 129	118	-110, 127	123
DCM_298K	-116, 129	115	-110, 129	121	-118, 130	112	-108, 131	121
DCM_350K	-113, 128	119	-114, 125	121	-116, 126	118	-112, 125	123
EA_298K	-114, 130	116	-117, 129	114	-115, 130	115	-121, 128	111
EA_350K	-113, 127	120	-117, 131	112	-119, 131	110	-114, 127	119
W_298K	-119, 130	111	-117, 131	112	-117, 131	112	-115, 130	115
W_350K	-117, 126	117	-115, 129	116	-119, 128	113	-118, 129	113
HE_298K	-116, 130	114	-107, 127	126	-113, 130	117	-113, 127	120
HE_350K	-118, 124	118	-112, 130	118	-112, 124	124	-114, 127	119
TOL_298K	-116, 129	115	-117, 130	113	-126, 131	103	-125, 133	102
TOL_350K	-117, 127	116	-116, 119	125	-119, 131	110	-117, 124	119
CH_298K	-115, 124	120	-113, 127	120	-116, 124	120	-109, 126	125
CH_350K	-112, 125	123	-109, 123	128	-116, 127	117	-113, 124	123

Note, D and S represent the distribution ranges and their spans, respectively. For example, under the condition of GAS_298K, D1 distributes two ranges of -180 to -113 and 120 to 180 degrees with D denoted as -113, 120. So its span (S) is [-113-(-180)]+[180-120]=127.

Table s6. Distribution fractional of *e* and *a*-formed NO_2 groups in the CL-20 conformations in solvents at 298 and 350 K.

Dihedrals	D1		D2		D3		D4	
	e	*a*	*e*	*a*	*e*	*a*	*e*	*a*
GAS_298K	0.61	0.39	0.60	0.40	0.59	0.41	0.59	0.41
GAS_350K	0.55	0.45	0.61	0.39	0.54	0.46	0.60	0.40
HE_298K	0.55	0.45	0.66	0.34	0.66	0.34	0.62	0.38
HE_350K	0.59	0.41	0.57	0.43	0.59	0.41	0.57	0.43
CH_298K	0.61	0.39	0.61	0.39	0.61	0.39	0.60	0.40
CH_350K	0.58	0.42	0.55	0.45	0.63	0.37	0.59	0.41
TCM_298K	0.55	0.45	0.62	0.38	0.59	0.41	0.62	0.38
TCM_350K	0.63	0.37	0.57	0.43	0.60	0.40	0.53	0.47
TOL_298K	0.79	0.21	0.73	0.27	0.73	0.27	0.70	0.30
TOL_350K	0.74	0.26	0.70	0.30	0.66	0.34	0.67	0.33

EA_298K	0.44	0.56	0.46	0.54	0.44	0.56	0.45	0.55
EA_350K	0.45	0.55	0.45	0.55	0.46	0.54	0.50	0.50
DCM_298K	0.63	0.37	0.61	0.39	0.59	0.41	0.61	0.39
DCM_350K	0.63	0.37	0.56	0.44	0.61	0.39	0.62	0.38
DCE_298K	0.54	0.46	0.51	0.49	0.55	0.45	0.54	0.46
DCE_350K	0.64	0.36	0.59	0.41	0.51	0.49	0.56	0.44
ACE_298K	0.43	0.57	0.44	0.56	0.48	0.52	0.50	0.50
ACE_350K	0.49	0.51	0.45	0.55	0.53	0.47	0.50	0.50
W_298K	0.52	0.48	0.54	0.46	0.46	0.54	0.47	0.53
W_350K	0.49	0.51	0.50	0.50	0.49	0.51	0.47	0.53